Research Square

Preprints are preliminary reports that have not undergone peer review.
They should not be considered conclusive, used to inform clinical practice,
or referenced by the media as validated information.

Vectorial Orientation of the Zygomaticus Major Muscle Using Facial Landmarks

Özlem Elvan

ozlemelvan@mersin.edu.tr

Mersin University

İsmail Yağmurhan Gilan[2]

Mersin University

Deniz Uzmansel

Mersin University

Alev Bobuş Örs

Mersin University

Research Article

Keywords: Zygomaticus major muscle, facial morphometry, facial landmarks, surgical anatomy

Posted Date: June 11th, 2026

DOI: https://doi.org/10.21203/rs.3.rs-9885960/v1

License: This work is licensed under a Creative Commons Attribution 4.0 International License.
Read Full License

Additional Declarations: No competing interests reported.

Abstract

Purpose

This study aimed to define the spatial localization and vectorial orientation of the zygomaticus major muscle (ZMM) using a combined linear and angular morphometric approach based on clinically relevant facial landmarks.

Methods

This descriptive cadaveric study was conducted on 22 formalin-fixed adult cadaveric heads. The origin, insertion, and midfiber direction of the ZMM were identified. A total of 14 linear and 5 angular parameters were measured. Reference lines were constructed between the lateral canthus, tragus, nasal wing, oral commissure, mandibular angle, and zygomatic arch. A proportional index was calculated as the ratio between the distance from the muscle origin to the lateral canthus and the distance between the lateral canthus and the tragus, to account for inter-individual facial size differences. Bilateral and sex-based comparisons, as well as correlation analyses, were performed.

Results

Linear measurements demonstrated no significant side or sex differences, indicating a high degree of bilateral symmetry in spatial relationships. In contrast, angular measurements showed greater variability, with a significant side difference observed only in the angle between the zygomatic arch and the muscle midfiber direction ($p = 0.034$). Moderate bilateral correlations were identified in selected linear parameters, whereas angular parameters showed limited correlation. The proportional index was 0.41 ± 0.07 on the right and 0.43 ± 0.08 on the left, with no significant differences between sides or sex. This finding indicated that the ZMM origin is consistently located at approximately two-fifths of the distance from the lateral canthus to the tragus.

Conclusion

The findings support a multi-landmark, multi-axial anatomical model of the ZMM. The proportional stability of this index and the symmetric linear organization provide a reliable framework for muscle localization, while angular variability highlights the importance of individualized vector assessment. This approach may enhance surgical planning in aesthetic and reconstructive procedures.

INTRODUCTION

Facial expression is produced through coordinated activity of the mimetic musculature, in which the zygomaticus major muscle (ZMM) functions as the principal elevator of the oral commissure during

smiling [16]. Because of its central contribution to midfacial movement and smile symmetry, the ZMM represents an important anatomical structure in aesthetic facial surgery, facial reanimation procedures, and superficial muscular aponeurotic system (SMAS)-based rhytidectomy techniques [4, 13, 15].

Anatomically, the ZMM originates from the lateral aspect of the zygomatic bone and inserts into the modiolus, blending with the orbicularis oris and SMAS. However, anatomical studies (Table 1) have demonstrated substantial interindividual variability in its morphology, attachment pattern, and course, including differences in muscle length, thickness, and configuration [1, 3, 10, 12, 16]. This variability increases the importance of reliable anatomical reference systems for clinical localization of the muscle.

Table 1
Morphometric Characteristics of the Zygomaticus Major Muscle Reported in the Literature

Study	Sample	Length (mm)	Width (mm)	Thickness (mm)	Angle (°)	Key Morphometric/ Topographic Findings
Pessa et al.1998	50 hemifaces	-	12 (6–20)	-	-	Bifid ZMM (34%) demonstrates superior and inferior bundles with distinct insertions, where the inferior slip may exhibit dermal attachment, creating a topographic basis for cheek dimple formation
Spiegel and DeRosa, 2005	48 hemifaces	-	-	-	-	The origin of the ZMM was identified 1.40–1.50 cm inferior to the Frankfort horizontal plane and approximately 1 cm lateral to the lateral canthus, at the level of the lateral canthus.
Farahvash et al. 2010	42 hemifaces 10 hemifaces	Single 61.3 ± 4.8 Each arm of bifid 55.3 ± 5.3/58.1 ± 6.5 bifid	Single 11 ± 2.8 Bifid 11.8 ± 2.1	-	-	Race-dependent midfacial variability; 19.2% bifid ZMM incidence.
Matic and Yoo, 2012	8 hemifaces	55 ± 7	-	-	51° ± 5°	Frankfort horizontal plane used as single reference axis

Study	Sample	Length (mm)	Width (mm)	Thickness (mm)	Angle (°)	Key Morphometric/ Topographic Findings
Zabojova et al., 2018	19 hemifaces	60.95 ± 6.9	6.5 ± 1.4	-	55.5°±12.6°	Horizontal plane used as single reference axis. Line of pull more oblique compared to levator muscles
Jacono et al., 2020	200 hemifaces (rhytidectomy patients)	-	-	-	59° ± 6° (41° – 72°)	Angle varies with age; high interindividual variability
Elvan et al., 2020	29 hemifaces	Upper margin: 47.52 ± 4.88 Lower margin: 55.19 ± 4.57 Lateral margin: 7.32 ± 1.90 Medial margin: 11.83 ± 3.64	-	2.69 ± 0.96	30.87° ±11.18° (10° – 50°)	Shapes of ZMM: Band-like (51%), fan-like (34%), bifid (13%) Variable relationship with orbicularis oculi muscle and parotid duct.
Sarilita et al., 2021	52 hemifaces (Thiel cadavers)	-	-	-	–	Origin at superior margin of temporal process on the lateral surface of zygomatic bone
Peer et al., 2022	10 hemifaces	-	-	-	Line-of-action analyzed in three-dimensional space	The findings underscore the need for three-dimensional structural knowledge in accurate vector planning for facial

Study	Sample	Length (mm)	Width (mm)	Thickness (mm)	Angle (°)	Key Morphometric/ Topographic Findings
						reanimation, yet they do not provide a clinically practical surface landmark–based framework.
Rams et al., 2024	34 healthy subjects	44.77 (31.8–55.6)	Origin 7.19 (3.6–13.3) Midportion 8.97 (4.9–14.8) Insertion 13.50 (2.8–32)	Origin 3.19 (1.3–6.1) Midportion 3.85 (1.2–6.8) Insertion 3.68 (1.0-7.3)	136.6° (105°-157°) Coronal plane used as single reference axis	Thickness is the most reliable parameter for functional assessment (repose, anger, joy, surprise, and sadness); increases during isotonic contraction.
Park et al., 2024	48 hemifaces	–	–		–	The ZMM origin is consistently located at the horizontal level of the nasal ala and vertically between the lateral canthus and tragus, with predictable surface landmark correlations

Previous morphometric investigations have primarily described the positional relationship of the ZMM with surface landmarks, particularly the lateral canthus, nasal wing, and tragus [1, 8]. These studies provide clinically useful information for identifying the muscle in surgical practice. In parallel, structural investigations have examined the relationship of the ZMM with the SMAS, facial nerve branches, and bony attachment sites, contributing to anatomical safety in midfacial procedures [7, 12, 15]. Despite these contributions, most anatomical descriptions remain position-based rather than vector-based, and the geometric orientation of the ZMM relative to multiple facial reference lines has not been comprehensively defined.

Quantitative studies addressing muscle orientation have generally relied on single-axis angular measurements. For example, Jacono et al. demonstrated considerable variability in ZMM orientation relative to horizontal reference planes, highlighting the limitations of standardized lifting vectors in facelift surgery [4]. Similarly, Zabojova et al. reported an oblique vector of pull for the ZMM, confirming that the muscle follows a consistent but variable oblique trajectory in the midface[16]. Imaging-based observations further indicate that angular changes in the ZMM reflect modiolus displacement and contraction behavior during facial movement [11], while functional studies suggest that skeletal and biomechanical changes can alter ZMM morphology and performance [5].

Together, these findings indicate that the ZMM should be understood as a vectorial anatomical structure, yet current anatomical literature does not provide a multi-reference angular model that can be applied in static anatomical conditions. In facial regions affected by trauma, reconstructive surgery, or tissue loss, reliance on a single anatomical landmark may be insufficient for accurate localization. Previous anatomical mapping studies have shown that multi-landmark reference systems and intersecting reference lines improve localization reliability when facial anatomy is altered [2]. Applying this principle to the ZMM suggests that defining the muscle using both linear distances and angular relationships between multiple facial landmarks may provide a more stable anatomical standard for clinical use. To date, no cadaveric morphometric study has systematically combined multi-landmark linear measurements with multi-axial angular analysis to describe the vectorial orientation of the ZMM using clinically relevant facial reference lines. Therefore, the aim of the present study was to define the anatomical position and vectorial orientation of the ZMM using reproducible facial landmarks through combined linear and angular morphometric analysis.

MATERIALS AND METHODS

This descriptive anatomical study was conducted on formalin-fixed adult cadaveric heads obtained from the Department of Anatomy, Faculty of Medicine, Mersin University. Specimens showing facial trauma, previous surgery, or marked facial asymmetry were excluded. The study included 22 cadaveric heads (11 male and 11 female). The mean age of the cadavers was 72.64 ± 13.60 years, and the mean head circumference was 56.19 ± 1.33 cm. All specimens were of Caucasian origin. Right and left hemifaces were evaluated separately.

The study was performed in accordance with institutional ethical standards and international guidelines for anatomical research using donated human bodies. Ethical approval was obtained from the Clinical Research Ethics Committee of Mersin University (2025/451).

After removal of the skin, subcutaneous tissue, and SMAS, the ZMM was exposed. The origin, muscle belly, and insertion were preserved. The dominant direction of the muscle midfibers was identified and marked to represent the contraction vector.

The following anatomical landmarks were identified: mandibular angle, tragus, oral commissure, nasal wing, lateral canthus, and zygomatic arch. Reference lines were constructed between these landmarks

(Fig. 1 and Fig. 2). The angular orientation of the ZMM was defined according to the dominant midfiber direction. Linear measurements were obtained using a digital caliper (precision: 0.01 mm). Angular measurements were performed using a surgical compass. All measurements were performed by the experienced anatomist.

Linear measurements

The following linear parameters were measured (Fig. 1):

L1: Distance from the intersection point of the ZMM midfiber line and the lateral canthus–mandibular angle line to the muscle origin along the midfiber direction

L2: Distance between the intersection point and the lateral canthus

L3: Distance between the intersection point and the mandibular angle

L4: Distance between the ZMM origin and the nasal wing

L5: Distance between the ZMM origin and the lateral canthus

L6: Distance between the ZMM origin and the mandibular angle

L7: Distance between the ZMM origin and the tragus

L8: Distance between the ZMM insertion and the mandibular angle

L9: Distance between the ZMM insertion and the lateral canthus

L10: Distance between the ZMM insertion and the nasal wing

L11: Distance between the lateral canthus and the tragus

L12: Distance between the lateral canthus and the mandibular angle

L13: Maximum length of the ZMM

L14: Width of the ZMM at the midpoint of the muscle belly

Additionally, the ratio between the origin–lateral canthus distance and the lateral canthus–tragus distance (L5/L11 ratio) was calculated.

Angular measurements

Angular measurements were defined between the ZMM midfiber direction and selected reference lines (Fig. 2):

A1: Angle between the zygomatic arch line and the ZMM midfiber direction

A2: Angle between the ZMM midfiber direction and the lateral canthus–mandibular angle line

A3: Angle between the lateral canthus–tragus line and the ZMM midfiber direction

A4: Angle between the oral commissure–tragus line and the ZMM midfiber direction

A5: Angle between the nasal wing–origin line and the nasal wing ZMM insertion line

Statistical Analysis

Statistical analyses were performed using statistical software. Normality of data distribution was evaluated using the Shapiro–Wilk test. Continuous variables were expressed as mean ± standard deviation, minimum, and maximum values. Independent sample t-tests were used for sex-based comparisons, and paired sample t-tests were used for side-to-side comparisons. Pearson correlation analysis was performed to evaluate relationships between right and left side measurements. Statistical significance was set at $p < 0.05$.

RESULTS

A total of 14 linear and 5 angular parameters were evaluated to characterize the localization of the ZMM. Linear measurements varied according to the anatomical reference points, with the lowest mean values observed in L14 and the highest in L12 on both sides. Similarly, angular measurements showed variability, with A4 representing the lowest and A1 the highest mean values bilaterally (Table 2).

Table 2

Linear morphometric and angular measurements of the zygomaticus major muscle according to side

Parameter	Right (Mean ± SD)	Left (Mean ± SD)	p	Total (Mean ± SD)
L1	11.74 ± 5.63 mm	12.68 ± 5.56 mm	0.621	12.22 ± 5.54 mm
L2	34.55 ± 5.47 mm	36.73 ± 5.27 mm	0.182	35.67 ± 5.41 mm
L3	64.08 ± 10.72 mm	62.14 ± 7.57 mm	0.444	63.09 ± 9.17 mm
L4	68.75 ± 7.13 mm	71.77 ± 7.19 mm	0.124	70.30 ± 7.23 mm
L5	35.54 ± 5.98 mm	35.97 ± 5.30 mm	0.837	35.76 ± 5.57 mm
L6	69.52 ± 9.28 mm	66.79 ± 8.79 mm	0.230	68.12 ± 9.02 mm
L7	56.42 ± 8.62 mm	52.83 ± 7.32 mm	0.151	54.58 ± 8.08 mm
L8	64.64 ± 9.55 mm	66.28 ± 6.30 mm	0.497	65.48 ± 7.98 mm
L9	61.60 ± 10.19 mm	57.62 ± 8.97 mm	0.088	59.56 ± 9.67 mm
L10	36.04 ± 7.23 mm	36.22 ± 7.20 mm	0.914	36.13 ± 7.12 mm
L11	88.03 ± 8.41 mm	85.30 ± 5.15 mm	0.083	86.63 ± 6.98 mm
L12	98.33 ± 8.52 mm	97.71 ± 7.65 mm	0.747	98.01 ± 7.98 mm
L13	55.76 ± 8.11 mm	57.22 ± 8.03 mm	0.546	56.51 ± 8.00 mm
L14	9.57 ± 3.33 mm	8.71 ± 2.13 mm	0.382	9.13 ± 2.78 mm
A1	135.12 ± 13.90°	143.06 ± 12.68°	0.034	–
A2	100.24 ± 9.64°	96.18 ± 10.31°	0.122	98.16 ± 9.96°
A3	115.12 ± 12.76°	114.47 ± 12.74°	0.855	114.79 ± 12.59°
A4	24.65 ± 8.80°	21.47 ± 7.99°	0.180	23.02 ± 8.38°
A5	51.76 ± 11.69°	51.18 ± 15.42°	0.864	51.46 ± 13.68°

The L5/L11 ratio was 0.41 ± 0.07 on the right side and 0.43 ± 0.08 on the left side, with no statistically significant difference between sides ($p = 0.423$). No significant differences were observed between gender.

Comparison between the right and left sides revealed no statistically significant differences in any linear parameters (L1 - L14; $p > 0.05$), indicating a high degree of bilateral symmetry in linear spatial relationships. Among angular measurements, only A1 demonstrated a statistically significant side difference ($p = 0.034$), with higher values observed on the left side and a moderate effect size (Cohen's $d = 0.60$) (Table 2).

Gender-based comparisons showed no significant differences in any linear or angular parameters ($p > 0.05$) (Table 3), suggesting that ZMM morphology and orientation are largely independent of gender in this

sample. Therefore, combined mean values independent of side were presented for overall sex-based evaluation.

Table 3
Gender based comparison of linear morphometric and angular measurements of the zygomaticus major muscle

Parameter	Male (Mean ± SD)	Female (Mean ± SD)	p
L1	11.56 ± 5.67 mm	12.03 ± 4.89 mm	0.742
L2	35.20 ± 6.52 mm	35.07 ± 3.91 mm	0.931
L3	64.97 ± 7.29 mm	61.78 ± 10.98 mm	0.284
L4	68.57 ± 6.95 mm	71.36 ± 7.03 mm	0.201
L5	34.14 ± 5.82 mm	36.53 ± 5.41 mm	0.183
L6	70.25 ± 7.03 mm	66.54 ± 10.63 mm	0.192
L7	55.12 ± 8.87 mm	52.90 ± 6.94 mm	0.366
L8	64.94 ± 7.46 mm	64.36 ± 9.67 mm	0.828
L9	60.16 ± 9.96 mm	58.55 ± 8.21 mm	0.560
L10	37.12 ± 7.28 mm	36.30 ± 6.99 mm	0.694
L11	86.33 ± 7.20 mm	85.20 ± 6.81 mm	0.592
L12	98.75 ± 7.08 mm	96.38 ± 9.71 mm	0.352
L13	55.71 ± 7.74 mm	55.75 ± 8.31 mm	0.986
L14	9.25 ± 2.96 mm	8.34 ± 2.52 mm	0.269
A1	133.40 ± 10.94°	141.78 ± 15.73°	0.061
A2	101.15 ± 9.95°	97.06 ± 9.49°	0.164
A3	112.73 ± 12.90°	115.89 ± 10.82°	0.377
A4	25.29 ± 9.12°	20.94 ± 5.68°	0.067
A5	53.95 ± 13.64°	47.72 ± 11.09°	0.102

Correlation analysis (Table 4) revealed moderate, positive relationships between the right and left sides for L6, L9, L10, L11, and L12, with the strongest correlation observed in L11 ($r = 0.693$, $p = 0.002$). In contrast, angular measurements showed limited bilateral correlation, with only A5 demonstrating a significant association ($r = 0.502$, $p = 0.040$).

Table 4
Significant correlations between right and left linear morphometric and angular measurements of the zygomaticus major muscle

Parameter	Pearson Correlation (r)	p
L6	0.502	0.040
L9	0.562	0.019
L10	0.552	0.022
L11	0.693	0.002
L12	0.537	0.026
A5	0.502	0.040
Linear measurements shown as (L): 1, distance from the intersection of the ZMM midfiber line and the lateral canthus–mandibular angle line to the muscle origin along the midfiber direction; 2, distance between the intersection point and the lateral canthus; 3, distance between the intersection point and the mandibular angle; 4, distance between the ZMM origin and the nasal wing; 5, distance between the ZMM origin and the lateral canthus; 6, distance between the ZMM origin and the mandibular angle; 7, distance between the ZMM origin and the tragus; 8, distance between the ZMM insertion and the mandibular angle; 9, distance between the ZMM insertion and the lateral canthus; 10, distance between the ZMM insertion and the nasal wing; 11, distance between the lateral canthus and the tragus; 12, distance between the lateral canthus and the mandibular angle; 13, maximum length of the ZMM; 14, width of the ZMM at the midpoint of the muscle belly.		
ZMM: zygomaticus major muscle; M: mandibular angle; C: lateral canthus; N: nasal wing; T: tragus, oral commissure.		
Angular measurements shown as (A): 1, angle between the zygomatic arch line and the ZMM midfiber direction; 2, angle between the ZMM midfiber direction and the lateral canthus–mandibular angle line; 3, angle between the lateral canthus–tragus line and the ZMM midfiber direction; 4, angle between the oral commissure–tragus line and the ZMM midfiber direction; 5, angle between the nasal wing–origin line and the nasal wing–insertion line of the ZMM.		
ZMM: zygomaticus major muscle; M: mandibular angle; C: lateral canthus; N: nasal wing; T: tragus; O: oral commissure.		

DISCUSSION

The present study provides a comprehensive linear and angular morphometric characterization of the ZMM using a standardized geometric reference system. A key finding of this study is that the L5/L11 ratio serves as a proportional parameter that accounts for inter-individual differences in facial size. Rather than relying on absolute measurements, this ratio defines the position of the ZMM origin in relative terms. Based on this proportional index, the ZMM origin is consistently located at approximately two-fifths of the lateral canthus–tragus distance from the lateral canthus.

Linear measurements defined the spatial relationships between the muscle's origin, insertion, and midfiber intersection point relative to stable craniofacial landmarks, including the lateral canthus, mandibular angle, nasal wing, and tragus. The distance from the intersection of the midfiber axis with the lateral canthus–mandibular angle line to the muscle origin (11.81 ± 5.31 mm) and to the lateral canthus (35.17 ± 5.40 mm)

indicates that the muscle can be localized using intersecting reference lines rather than a single landmark. Similarly, origin–nasal wing (69.89 ± 7.11 mm), origin–lateral canthus (35.23 ± 5.66 mm), insertion–lateral canthus (64.67 ± 8.46 mm), and insertion–mandibular angle (59.34 ± 9.16 mm) distances showed reproducible relationships with both perioral and lateral facial reference points. Baseline distances such as lateral canthus–tragus (85.76 ± 6.99 mm) and lateral canthus–mandibular angle (97.64 ± 8.42 mm) further support the structural stability of the coordinate system. Angular measurements provided complementary evidence for the oblique vectorial orientation of the muscle. The angles between the zygomatic arch line and the midfiber direction (left: 143.06 ± 12.68°, right: 135.12 ± 13.90°; p = 0.034°), and between the midfiber and the lateral canthus–mandibular anglee line (99.23 ± 9.88°), demonstrated a consistent orientation pattern. Additional angles relative to clinically relevant axes, including the lateral canthus–tragus (114.18 ± 12.04°) and oral commissure–tragus (23.23 ± 7.99°) lines, confirmed functional alignment with facial expression mechanics. The nasal wing–origin and nasal wing–insertion angle (51.10 ± 12.86°) further illustrated the geometric relationship of the muscle attachments within the perinasal region. Together, these findings demonstrate a predominantly symmetric linear organization of the ZMM across the midface, accompanied by greater variability in angular parameters. While the absence of significant side differences and the presence of moderate bilateral correlations in linear measurements suggest a stable spatial framework for muscle localization, the observed asymmetry between the zygomatic arch line and the ZMM midfiber direction (A1) and the limited correlations among angular parameters indicate that muscle orientation is more variable than its linear positioning.

Previous studies (Table 1) have primarily focused on descriptive positional anatomy [1, 8, 13] or on single-axis angular measurements relative to the Frankfort horizontal plane [4, 16]. Structural and neuroanatomical studies have further clarified surgical safety and innervation patterns [12, 15]; however, these studies did not quantify vectorial orientation. Although these studies contributions have improved anatomical localization, they have not integrate multiple spatial references. Clinically, accurate definition of ZMM orientation is particularly relevant in SMAS-based facelift techniques, where lifting vectors not aligned with the native muscle direction may result in unnatural facial expression [4, 7]. Jacono et al. demonstrated significant interindividual variability and age-related changes in ZMM orientation, underscoring the need for individualized landmark-based reference models rather than assumed standard vectors [4]. Matic and Yoo quantified ZMM orientation using a single angular axis relative to the Frankfort horizontal plane [6], whereas the present study incorporates multiple anatomical reference lines within a structured geometric system.

The methodology of the present study is consistent with current facial mapping approaches that use multiple anatomical landmarks rather than relying on a single reference line. In parotid duct localization studies, multi-line reference systems demonstrated that anatomical structures do not consistently follow a single surface line, requiring intersecting reference axes for reliable localization [14]. Similarly, spatial mapping of the facial artery and vein showed that combining linear and angular measurements relative to multiple landmarks improves anatomical precision and clinical applicability [2]. Applied to the ZMM, this multi-axial model defines the muscle vector in relation to multiple clinically relevant landmarks, improving reliability in cases of soft tissue distortion, prior surgical intervention or anatomical variation.

Understanding the angular and linear relationships of the ZMM has direct clinical relevance in both aesthetic and reconstructive procedures. In facial reanimation surgery, accurate replication of the native muscle vector and length is essential for achieving a symmetric and natural smile. In filler and botulinum toxin applications, knowledge of the muscle's origin, insertion, and its relationship to surface landmarks such as the nasal wing and lateral canthus helps guide injection depth and location, reducing the risk of asymmetry or unintended muscle involvement. During midface lift procedures, awareness of the muscle's orientation relative to common reference lines supports appropriate vector planning and preservation of natural facial dynamics. Overall, a landmark-based angular framework allows anatomical findings to be translated more reliably into clinical decision-making.

Accurate surgical planning requires understanding the three-dimensional architecture and native vector of the ZMM. Inadequate knowledge of muscle line-of-action may lead to non-physiological movement and suboptimal aesthetic outcomes [9]. Although detailed three-dimensional modeling provides precise architectural guidance, it is not always feasible in routine practice. Therefore, integrating vectorial orientation with surface-based morphometric landmarks may offer a practical anatomical guide for reconstructive surgeons.

From a surgical perspective, defining the ZMM through a multi-landmark angular framework may improve intraoperative orientation during SMAS-based rhytidectomy, midface lifting, and facial reanimation procedures, where alignment with the native muscle vector is critical for preserving natural smile dynamics. Such a framework may assist surgeons in vector planning, muscle transfer positioning, and injection-based treatments by offering reproducible surface correlations. Nevertheless, several limitations should be acknowledged. The cadaveric sample had a relatively advanced mean age, and age-related sarcopenic changes may influence muscle morphology and angular orientation. Additionally, formalin fixation may alter soft tissue elasticity and dimensional accuracy. The study population consisted of Caucasian specimens, which may limit generalizability across different ethnic groups. Future investigations incorporating younger specimens, imaging-based validation, and functional correlation studies are warranted to confirm the clinical transferability of this anatomical model.

Conclusion

The present study demonstrates that the ZMM can be defined through a multi-reference, landmark-based linear and angular framework. The consistent spatial, angular, and proportional relationships identified support the reliability of intersecting reference lines for muscle localization. This vector-based coordinate model offers an anatomically grounded and clinically applicable approach for understanding ZMM orientation in both aesthetic and reconstructive facial surgery.

Declarations

Ethical approval:

The present study was approved by Mersin University, Ethics Board of Clinical Research (2025/451). This study conforms to recognized standards of Helsinki Declaration

Conflict of interest:

The authors declare no conflicts of interest.

Funding information:

No funding.

Author Contribution

ÖE: Project development, Manuscript writing/editing, Data collection, Data analysisDU: Project development, Manuscript writing/editingABÖ: Project development, Manuscript writing/editingİYGilan: Data collection, Data analysis

Acknowledgements:

We would like to acknowledge the use of a large language model to assist with refining language, improving grammatical clarity, and suggesting alternative phrasing during the preparation of this manuscript. The authors critically reviewed and significantly revised all generated content to ensure accuracy, originality, and adherence to academic standards.

Data availability:

Details of the study are provided within the manuscript. Further inquiries can be directed to the corresponding author.

References

1. Elvan Ö, Bobuş Örs A, Tezer MS (2020) Anatomical evaluation of zygomaticus major muscle with relation to orbicularis oculi muscle and parotid duct. J Craniofac Surg 31:1844–1847. https://doi.org/10.1097/SCS.0000000000006396
2. Elvan Ö, Uzmansel D (2025) Mapping the localization of the facial artery and vein at the inferior border of the mandible for clinical applications. Anat Sci Int 100:280–286. https://doi.org/10.1007/s12565-024-00806-1
3. Farahvash MR, Abianeh SH, Farahvash B et al (2010) Anatomic variations of midfacial muscles and nasolabial crease: a survey on 52 hemifacial dissections in fresh Persian cadavers. Aesthet Surg J

30:17–21

4. Jacono AA, Bryant LM, Alemi AS (2020) Optimal facelift vector and its relation to zygomaticus major orientation. Aesthet Surg J 40:351–356. https://doi.org/10.1093/asj/sjz114
5. Kohara R, Gomi K, Shin YM, Moroi A, Yoshizawa K, Ueki K (2025) Evaluation of zygomaticus major muscle and lip-closing force in orthognathic surgery: retrospective study. Maxillofac Plast Reconstr Surg 47:10. https://doi.org/10.1186/s40902-025-00466-9
6. Matic DB, Yoo J (2012) The pedicled masseter muscle transfer for smile reconstruction in facial paralysis: repositioning the origin and insertion. J Plast Reconstr Aesthet Surg 65:1002–1008. https://doi.org/10.1016/j.bjps.2012.03.021
7. Mowlavi A, Wilhelmi BJ (2004) The extended SMAS facelift: identifying the lateral zygomaticus major muscle border using bony anatomic landmarks. Ann Plast Surg 52:353–357. https://doi.org/10.1097/01.sap.0000099712.80882.6b
8. Park HJ, Park JS, Iwanaga J, Tubbs RS, Hur MS (2024) Positional relationships of the origin and course of zygomaticus major with the nasal ala, tragus, philtrum, and lateral canthus for aesthetic treatments and surgeries. Surg Radiol Anat 46:27–32. https://doi.org/10.1007/s00276-023-03271-z
9. Peer M, Tran J, Li Z, Fattah AY, Agur AMR, Davies JC (2022) Parametric multi-scale modeling of the zygomaticus major and minor: implications for facial reanimation. J Craniofac Surg 33:701–706. https://doi.org/10.1097/SCS.0000000000008128
10. Pessa JE, Zadoo VP, Garza PA et al (1998) Double or bifid zygomaticus major muscle: anatomy, incidence, and clinical correlation. Clin Anat 11:310–313
11. Rams DJ, Alfertshofer M, Batko J, Gotkin RH, Perdikis G, Szczepanek E, Urbanik A, Koziej M, Ostrogórska M, Cotofana S (2024) Investigating the contraction pattern of the zygomaticus major muscle and its clinical relevance: a functional MRI study. Aesthetic Plast Surg 48:2722–2729. https://doi.org/10.1007/s00266-024-03876-8
12. Sarilita E, Rynn C, Mossey PA, Black S (2021) Zygomaticus major muscle bony attachment site: a Thiel-embalmed cadaver study. Morphologie 105:24–28. https://doi.org/10.1016/j.morpho.2020.06.009
13. Spiegel JH, DeRosa J (2005) The anatomical relationship between the orbicularis oculi muscle and the levator labii superioris and zygomaticus muscle complexes. Plast Reconstr Surg 116:1937–1942. https://doi.org/10.1097/01.prs.0000189194.86005.4b
14. Uzmansel D, Elvan Ö, Aktekin M (2022) Precise localization of parotid duct: a cadaveric study. Anat Sci Int 97:59–64. https://doi.org/10.1007/s12565-021-00626-7
15. Yoshioka N, Fernandez-Miranda JC (2024) Nerve to the zygomaticus major muscle: an anatomical study and surgical application to smile reconstruction. Clin Anat 37:376–382. https://doi.org/10.1002/ca.24079
16. Zabojova J, Thrikutam N, Tolley P, Perez J, Rozen SM, Rodriguez-Lorenzo A (2018) Relational anatomy of the mimetic muscles and its implications on free functional muscle inset in facial reanimation. Ann Plast Surg 81:203–207. https://doi.org/10.1097/SAP.0000000000001507

Figures

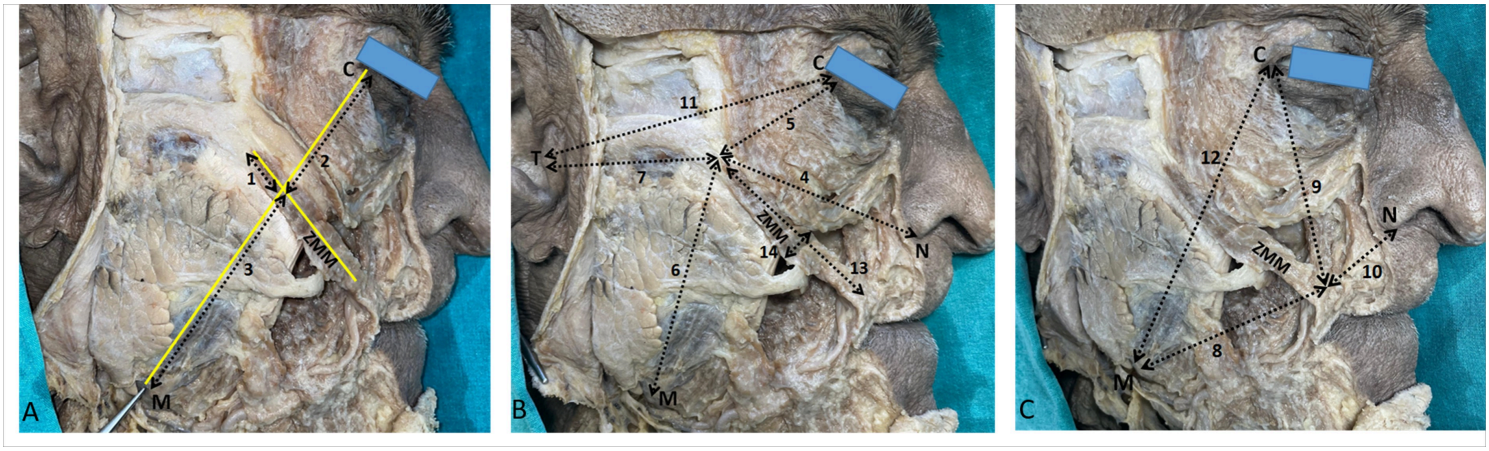


Figure 1

Cadaveric photo showing the linear morphometric measurements of the zygomaticus major muscle.

Linear measurements shown as (L): 1, distance from the intersection of the ZMM midfiber line and the lateral canthus–mandibular angle line to the muscle origin along the midfiber direction; 2, distance between the intersection point and the lateral canthus; 3, distance between the intersection point and the mandibular angle; 4, distance between the ZMM origin and the nasal wing; 5, distance between the ZMM origin and the lateral canthus; 6, distance between the ZMM origin and the mandibular angle; 7, distance between the ZMM origin and the tragus; 8, distance between the ZMM insertion and the mandibular angle; 9, distance between the ZMM insertion and the lateral canthus; 10, distance between the ZMM insertion and the nasal wing; 11, distance between the lateral canthus and the tragus; 12, distance between the lateral canthus and the mandibular angle; 13, maximum length of the ZMM; 14, width of the ZMM at the midpoint of the muscle belly.

ZMM: zygomaticus major muscle; M: mandibular angle; C: lateral canthus; N: nasal wing; T: tragus, oral commissure.

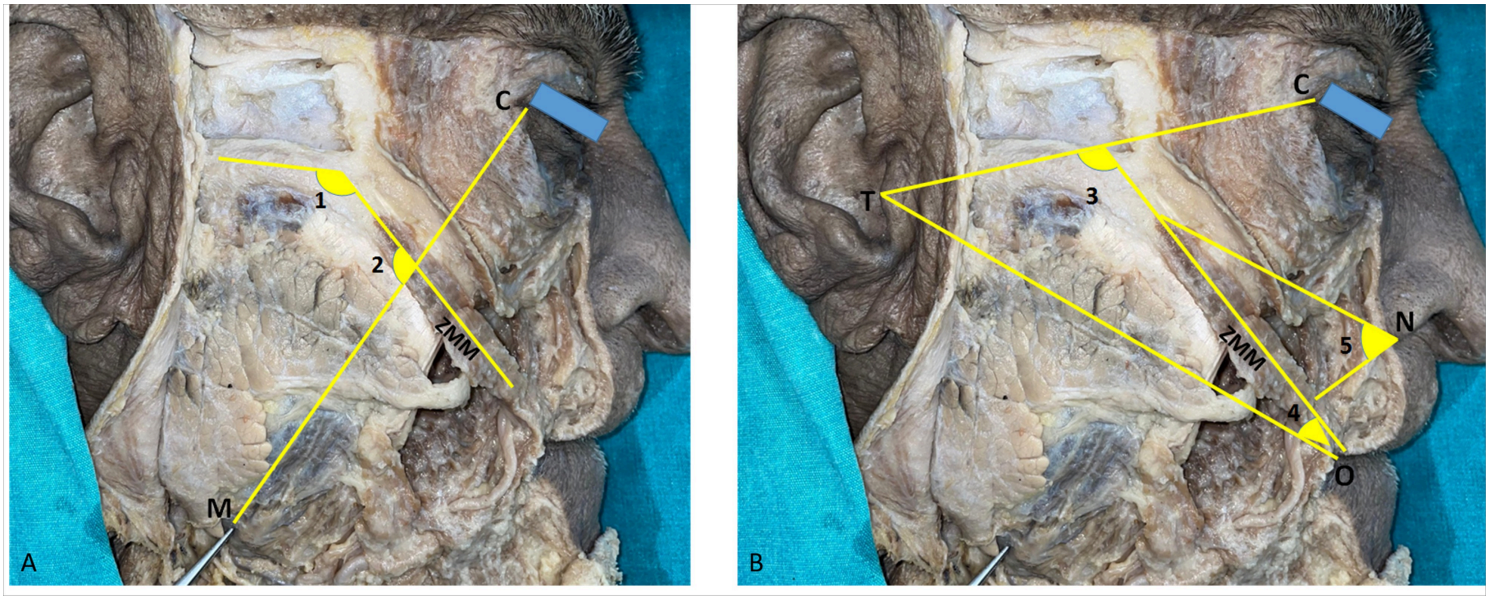


Figure 2

Cadaveric photo showing the angular morphometric measurements of the zygomaticus major muscle.

Angular measurements shown as (A): 1, angle between the zygomatic arch line and the ZMM midfiber direction; 2, angle between the ZMM midfiber direction and the lateral canthus–mandibular angle line; 3, angle between the lateral canthus–tragus line and the ZMM midfiber direction; 4, angle between the oral commissure–tragus line and the ZMM midfiber direction; 5, angle between the nasal wing–origin line and the nasal wing–insertion line of the ZMM.

ZMM: zygomaticus major muscle; M: mandibular angle; C: lateral canthus; N: nasal wing; T: tragus; O: oral commissure.